Performance Analysis of a Double-pass Thermoelectric Solar Air Collector

C. Lertsatitthanakorn [a,*], N. Khasee [a], S. Atthajariyakul [a], S. Soponronnarit [b],

A. Therdyothin [b], Ryosuke O. Suzuki [c]

[a] Faculty of Engineering, Mahasarakham University, Khantarawichai, Mahasarakham 44150, Thailand

[b] School of Energy, Environment and Materials, King Mongkut's University of Technology Thonburi, Bangmod, Thungkru, Bangkok 10140, Thailand

[c] Engineering of Eco-Processing Laboratory, Department of Material Science, Hokkaido University, Sapporo, Hokkaido 0600809, Japan

Abstract

The thermoelectric (TE) solar air collector, sometimes known as the hybrid solar collector, generates both thermal and electrical energies simultaneously. A double pass TE solar air collector has been developed and tested. The TE solar collector was composed of transparent glass, air gap, an absorber plate, thermoelectric modules and rectangular fin heat sink. The incident solar radiation heats up the absorber plate so that a temperature difference is created between the thermoelectric modules that generate a direct current. Only a small part of the absorbed solar radiation is converted to electricity, while the rest increases the temperature of the absorber plate. The ambient air flows through the heat sink located in the lower channel to gain heat. The heated air then flows to the upper channel where it receives additional heating from the absorber plate. Improvements to the thermal and overall efficiencies of the system can be achieved by the use of the double pass collector system and TE technology. Results show that the thermal efficiency increases as the air flow rate increases. Meanwhile, the electrical power output and the conversion efficiency depended on the temperature difference between the hot and cold side of the TE modules. At a temperature difference of 22.8°C, the unit achieved a power output of 2.13 W and the conversion efficiency of 6.17%. Therefore, the proposed TE solar collector concept is anticipated to contribute to wider applications of the TE hybrid systems due to the increased overall efficiency.

Keywords: Thermal efficiency; Conversion efficiency; Overall efficiency; Power output

1. Introduction

Every energy generation and transmission method affects the environment. It is obvious that conventional generating options can damage air, climate, water, land and wildlife, landscape, as well as raise the levels of harmful radiation. Renewable technologies are substantially safer offering a solution to many environmental and social problems associated with fossil and nuclear fuels. Solar energy is one type of renewable energy, which provides obvious environmental advantages in comparison to conventional energy sources, thus contributing to the sustainable development of human activities [1]. Not counting the depletion of the exhausted natural resources solar energy's main advantage is related to reducing CO_2 emissions, and normally it is absent of any air emissions or waste products during operation. Solar energy has the potential to meet a significant proportion of the world's energy needs [2]. It can be broadly classified into two systems; a thermal energy system which converts solar energy into thermal energy and an electrical system which converts solar energy into electrical energy. Normally, these two collection systems are used separately. It has been shown that these systems can be combined to form a hybrid photovoltaic-thermal (PVT) systems. The heat accumulated in the solar cells is recovered in the form of low temperature thermal energy, resulting in improvements in the electrical conversion efficiency of PV modules. Over the last few years, difference PVT systems, based on air and water as heat carrying fluid, have been studied, developed and reported in literature. As the example, Kalogirou [3] has studied experimentally an unglazed hybrid PVT system under the force mode of operation for climatic condition of Cyprus. He observed an increase in the mean annual efficiency of a PV solar system from 2.8% to 7.7% with a thermal efficiency of 49%. Hagazy [4] and Sopian et al. [5] investigated a glazed PVT air system for a single and double pass air heater for space heating and drying purposes. They have also developed a thermal model of each system. Thermal energy for the glazed PVT system is increased with lower electrical efficiency due to high operating temperature. However, there is another technology for combined electrical and thermal energies namely: thermoelectric (TE) technology. The term TE refers to solar thermal collectors that use TE devices as an integral part of the absorber plate. The system generates both thermal and electrical energy simultaneously.

A TE device for power generation consists of n and p semiconductors connected electrically in series and thermally in parallel. Heat is supplied at one end of the TE, while the other end is maintained at a lower temperature with a heat sink [6]. As a result of the temperature difference, a current flows through an external load resistance. TE has the advantage that it can operate from a low grade heat source such as waste heat energy. It is also attractive as a means of converting solar energy into electricity. A number of simulations as well as experimental studies have been reported on solar-driven TE power generators. Chen [7] derived a thermodynamic analysis of solar-driven TE power generator based on a well-insulated flat plate collector. A thermodynamic model including four irreversibilities is used to investigate the optimum performance of a solar-driven TE generator. The example discussed by Chen is based on an extremely well-insulated flat plate collector, which, in practice, may be difficult to achieve. Gunter et al. [8] constructed a prototype of a solar thermoelectric water heater. The hot side of TE module was heated by solar hot water. Meanwhile, the heat was released at the cold side of TE module via a heat sink. Three vacuum-tubes with heat pipes, each with a 0.1 m^2 absorber area and with water as the heat pipe medium, were connected via a specially designed heat exchanger to a fluid circuit acting as a heat sink. Test result showed that the electrical efficiency reached a maximum value of 1.1% of the incoming solar radiation, which is around 2.8% of the transferred heat. Scherrer et al. [9] presented a series of mathematical models based on the optimal control theory to asses the electric performance of a skutterudites-based solar TE generator as a function of sun-spacecraft distance, and optimized its design parameters (such as dimensions, weight and so on) when operating at a distance of 0.45 a.u. from the sun, for 400 W electrical output power and for a required load voltage of 30 VCD. The simulation results indicated that the skutterudites-based solar TE generator offered attractive performance features as primary or auxiliary power source for spacecraft in near-Sun missions. Maneewan et al. [10] studied a thermoelectric roof solar collector (TE-RSC) to reduce roof heat gain and improve indoor thermal comfort. Maneewan’s TE-RSC combined the advantages of a roof solar collector and TE to act as a power generator. The electric current produced by the TE modules was used to run a fan for cooling the modules and improve the indoor thermal conditions. The subsequent simulation results, using a real house configuration, showed that a TE-RSC unit with a 0.0525 m^2 surface area could generate about 1.2 W under solar radiation intensity of about 800 W/m^2 and at ambient temperatures varying between 30 and 35°C. The induced air change rate varied between 20 and 45 ACH (Number of air changes per hour) and the corresponding ceiling heat transfer rate reduction was about 3-5 W/m^2. The electrical conversion efficiency of the proposed TE-RSC system is 1-4%.

In this work, an attempt has been made to develop and test a TE solar air heater to study the performance under the tropical climate of Mahasarakham, Thailand.

2. Analysis

The thermal output Q_{th} and electrical output P of the TE solar collector are calculated from the measured data as follows:

$$Q_{th} = mC_p\left(T_{aco} - T_{amb}\right) \tag{1}$$

$$P = I_{mp} \cdot V_{mp} \tag{2}$$

where C_p is the specific heat at the average air temperature, m is the air mass flow rate, T_{aco} and T_{amb} are the air temperature at the outlet of collector and ambient temperature, respectively. I_{mp} and V_{mp} are the maximum current and voltage of the TE modules at a matched load.

Theoretically, the maximum power output of a realistic TE module takes into account the contact resistance as given by [11].

$$P = \frac{\alpha^2}{2\rho} \frac{NA\left(T_h - T_c\right)^2}{\left(L + n\right)\left(1 + 2rL_c / L\right)^2} \tag{3}$$

where T_h and T_c are the hot side and cold side of thermoelectric, respectively.

Typically, n = 0.1 mm, r = 0.2, L = 1.2 mm, L_c = 0.8 mm, α = 2.1226 x 10^{-4} $V.K^{-1}$, N= 127 couples, ρ = 2.07 x 10^{-3} Ω.cm and A = 1.96 mm^2.

The heat released from the heat sink at the cold side of TE modules is calculated from:

$$Q_w = mC_p\left(T_{aho} - T_{amb}\right) \quad (4)$$

where T_{aho} is the air temperature at the outlet of heat sink

The performance of a TE solar collector can be described by a combination of efficiency terms. The basic ones are the thermal efficiency η_{th} and the conversion efficiency η_c are calculated based on the following definition:

$$\eta_{th} = \frac{Q_{th}}{A_a G} \quad (5)$$

$$\eta_c = \frac{P}{A_{TE} G} \quad (6)$$

where A_a is the aperture area of absorber plate, A_{TE} is the area of TE modules and G is the incident solar radiation.

The total efficiency η_o is commonly used to assess the overall performance

$$\eta_o = \frac{\left(Q_{th} + P - P_b\right)}{A_a G} \quad (7)$$

where P_b is blower power.

3. Description of the TE solar collector and experimental methodology

The schematic view of the TE solar collector is shown in Figure 1. The TE solar collector was composed of a glass cover, air gap, galvanized iron plate and TE modules with the hot side attached directly to the back side of the galvanized iron plate acting as absorber, and rectangular fin heat sink directly attached to the cold side of the TE modules. The space between the TE modules, absorber and heat sink was insulated using the closed cell elastomeric thermal insulator (thermal conductivity = 0.039 W/mK). The collector was 1 m wide, 1.5 m long, with an aperture area of 1.5 m^2. It also had a 0.11 m flow duct height (air gap), leading to a flow area of 0.11 m^2. The absorbing sure surface in the collector was made of galvanized iron, 2.5 mm thick, painted with dull black. Twenty four TE cooling (model TEC1—12708, China) modules are made of bismuth telluride based alloys were used. Each module had an area of 4 x 4 cm^2. The TE modules were connected in series and arranged in 4 rows with 6 TE modules in each row. The rectangular fin heat sink on the cold side was made of aluminum. The fins were 4.5 mm thick; 120 mm long in the horizontal direction and had a height of 40 mm from the base with a fin space of 7 mm. A centrifugal blower was used to circulate the air through the rectangular fin heat sink and the collector. The collector was oriented to south and tilted so as to adjust an angle of 16° from horizontal, which was considered suitable for the geographical location of Mahasarakham, Thailand (16°14′N, 103°15′E) [12].

Ambient air enters the lower channel and captures released heat from the heat sink located at the cold side of TE modules. Next it enters the upper channel where it is further heated by the absorber plate. The air temperature at the outlet of the collector is at a high temperature because it is using the recycled air form the lower channel. This concept was to improve the thermal efficiency of the flat plate collector and obtain electrical power from the TE as well.

The collector was instrumented with T-type (accuracy ±0.5°C) thermocouples for the glass cover, the flowing air, the surface of absorber plate and heat sink as shown in Figure 1. The thermocouple, which measured the ambient temperature, was kept in a shelter to protect the sensor from direct sunlight. A pryanometer (Kipp & Zonen model CM 11 accuracy ±10 W/m^2) was used to measure the incident solar radiation. The air flow rate was calculated from the air velocity, measured by a hot wire anemometer (Testo model 445, accuracy ±0.03 m/s) at the collector outlet, and the known duct area. The output current and voltage were measured with a multi-meter (Fluke model 189, accuracy VDC ±0.025%, A ±0.5%). The experiments were performed during June 2007. Experimentation started at 9 a.m. and ended at 5 p.m.

4. Results and discussion

4.1 Thermal performance of the TE solar collector

The variations of incident solar radiation (G), ambient temperature (T_{amb}), air temperature at the outlet of the heat sink (T_{aho}) and the collector (T_{aco}) for air flow rate of 0.054 kg/s are shown in Fig. 2. The variation of ambient air temperature varied from 29.7 to 35.3°C while the air temperature at the outlet of the heat sink varied from 31.4 to 49.7°C. During the test period, the air temperature at the outlet of the heat sink was higher than the ambient air temperature. This is due to heat rejected from the heat sink to the flowing air. Consequently, the air temperature at the outlet of the collector, which heats up the recycled air from the outlet of the heat sink, was observed to be much higher than the ambient. The maximum temperature rise was 17.9°C at the incident solar intensity of 876 W/m^2.

The effect of increasing the air mass flow rate on the absorber plate (T_{abs}), cover plate (T_{cov}) and air temperature of the outlet of the collector is presented in Fig. 3. It is apparent, as expected, that as the air mass flow rate increases the air temperature at the outlet of the collector decreases. Further, for high air mass flow rates, the collector operating temperature would be lower, resulting in lower heat losses and subsequently, higher thermal efficiency. It can be seen that the thermal efficiency of the air collector is strongly dependent on the air flow rate. The efficiency increased constantly up to 0.088 kg/s and tended to approach a constant value. The maximum thermal efficiency was 80.3% corresponding to the air flow rate of 0.123 kg/s and incident solar radiation of 950.7 W/m^2 as shown in Fig. 4. In all of the results, it was observed that the temperature of the absorber plate exhibits the highest temperature and the temperature of the glass cover the lowest. As the air flow rate increases, the temperature differences between the air and absorber plate decreases. Fig. 5 shows the maximum rise in air temperature $(T_{aco} - T_{amb})_{max}$ is seen to drop as expected with increasing mass flow rate. This range of flow rates will give an outlet temperature suitable for most agricultural drying application, and the corresponding efficiency is considered reasonable [13].

4.2 Electrical and overall performances of the TE solar collector

Fig. 6 presents the output power and conversion efficiency, as a function of temperature difference between hot and cold sides of the TE modules. It is apparent that the power and efficiency continued to increase as the temperature difference increased. The maximum power and conversion efficiency are 2.13 W and 6.17%, respectively at a temperature difference of 22.8°C. The open-circuit voltage and the short-circuit current are 10.05 V and 212.56 mA, respectively. Data obtained from the experiment was used to validate the TE model presented. In Fig. 7, the predicted and measured power delivered into a matched load as a function of temperature difference between hot and cold side of the TE modules are compared. The power was proportional to the product of the square of the temperature difference and the square of the Seebeck coefficient, so that as the temperature difference increased, the term primarily determined the power output [14]. The decrease in Seebeck coefficient, which had been incorporated into the model and based on published data, was too small to compensate for this increase. However, at low temperatures, there was positive agreement between the predicted power and measurement. Consequently, the level of agreement between the model and the measured data was encouraging and gave confidence in the accuracy of the model, at least under the operational conditions investigated. The effect of air flow rate on the rate of withdrawal of heat from the cold side of the TE modules has been shown in Fig. 8. It can be observed that the rate of withdrawal of heat increases as the air flow rate increases. The rate of withdrawal of heat from the cold side of the TE modules can be obtained from Eq. (4). The higher heat rejection from the cold side of TE gives the greater power output [15]. Effect of air flow rate on conversion and overall efficiencies has been shown in Fig. 9. The conversion efficiency slightly decreases with increases of air flow rate. Generally, the overall efficiency increases with an increase in air flow rate, attains a maximum value and then decreases with a further increase in air flow rate. This is attributed to the sharp increase in blower power with increasing air flow rate.

5. Conclusions

The TE solar collector technology provides a solution to improving the energy yields per unit surface area of a solar collector. The TE solar air heater approach is particularly suitable for most agricultural drying applications. We used air as a flowing fluid to extract heat from the TE modules and to improve the thermal efficiency of the solar collector. The results showed that the TE solar collector generates electrical power of 2.13 W at the temperature difference of 22.8°C. The thermal efficiency increases with increasing air flow rate. The maximum thermal efficiency was 80.3% at the air flow rate of 0.123 kg/s, the electrical efficiency around 5.7%. Meanwhile, the maximum overall efficiency was 72.22% at the air flow rate of 0.088 kg/s. The proposed theoretical model may be used for predicting the output power of the TE modules with reasonable accuracy given temperature difference conditions.

Acknowledgements

The authors are grateful to the Thailand Research Fund (TRF) and the Commission of Higher Education of the Ministry of Education for providing financial support. Experimental help of Mr. Pravit Phumkhet and Mr. Teerawat Passasai is highly appreciated.

References

[1] T. Tsoutsos, N. Frantzeskaki V. Gekas, Energy Policy 33 (2005) 289.

[2] M.Y.Hj. Othman, B. Yatim, K. Sopian, M.N.A. Bakar, Renew. Energy 30 (2005) 2005.

[3] S.A. Kalogirou, Renew. Energy 23 (2001) 247.

[4] A.A. Hegazy, Energy Convers. Manage. 41 (2000) 861.

[5] K. Sopin, H.T. Liu, S. Kakac, T.N. Veziroglu, Energy Convers. Manage. 41 (2000) 353.

[6] D.M. Rowe, Renew. Energy 16 (1999) 1251.

[7] J. Chen, J. Appl. Phy. 79 (1996) 2717.

[8] R. Gunter, Sol. Energy 67 (1999) 227.

[9] H. Scherrer, L. Vikhor, B. Lenior, A. Dauscher, P. Poinas, J Power Sources 115 (2003) 141.

[10] S. Maneewan, J. Hirrunlabh, J. Khedari, B. Zeghmati, S. Teekasap, Sol Energy 78 (2005) 495.

[11] C. Lertsatitthanakorn, Bioresource Technology 98 (2007) 1670.

[12] S. Pattanasethanon, C. Lertsatitthanakorn, S. Atthajariyakun, S. Soponronnarit, Energy Convers. Manage. 48 (2007) 1601.

[13] M.A. Karim, M.N.A. Hawlader, Energy Convers. Manage. 45 (2004) 329.

[14] S.A. Omer, D.G. Infield, Sol. Ener. Mat. Sol. Cells 53 (1998) 67.

[15] R.Y. Nuwayhid, A. Shihadeh, N. Ghaddar, , Energy Convers. Manage. 46 (2005) 1631.

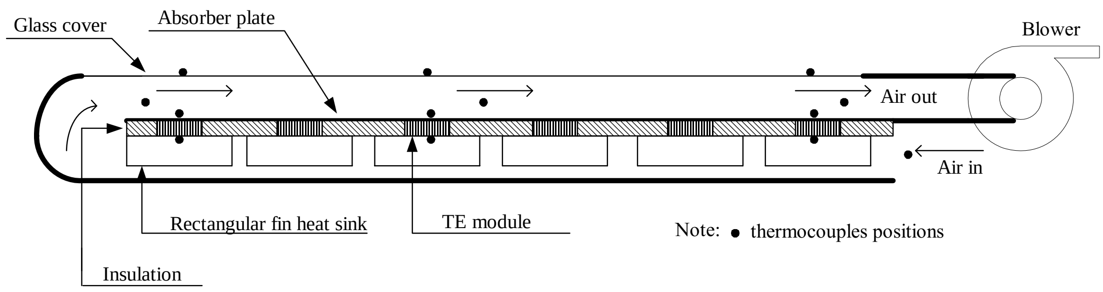

Fig. 1. A schematic diagram of the TE solar air collector

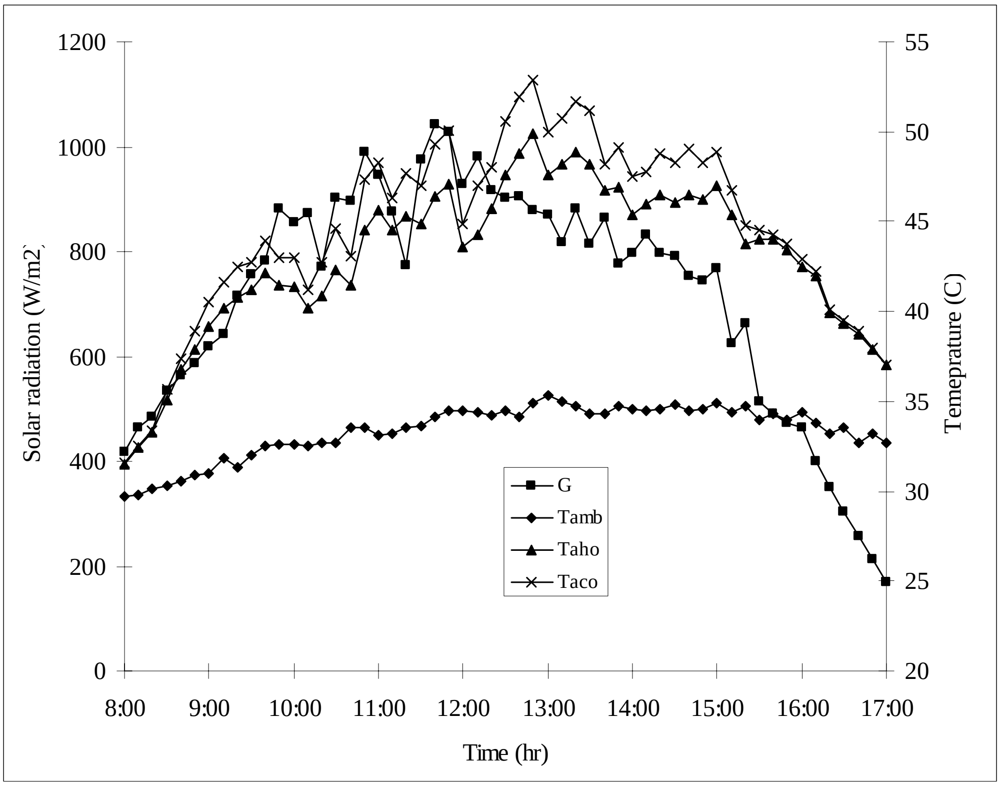

Fig. 2. Variations of incident solar radiation, ambient temperature, average air temperature of outlet heat sink and collector. (Air flow rate of 0.054 kg/s, 6 June 2007)

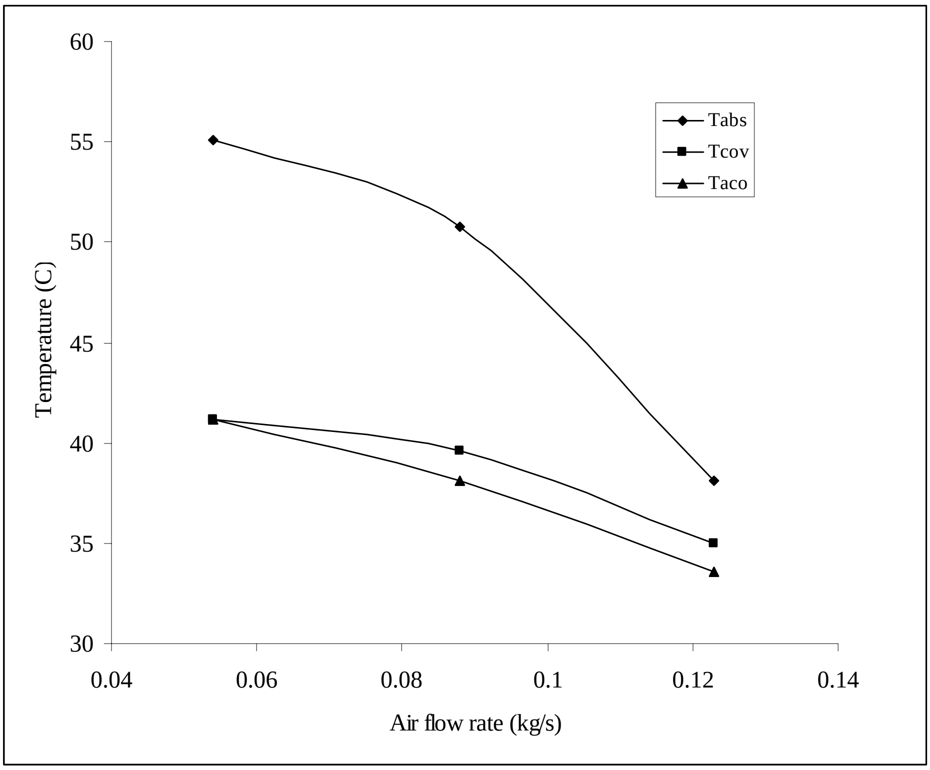

Fig. 3. Effect of air flow rate on the temperature of absorber plate and cover plate and air temperature of the outlet of the collector (Incident solar radiation of 650 W/m^2)

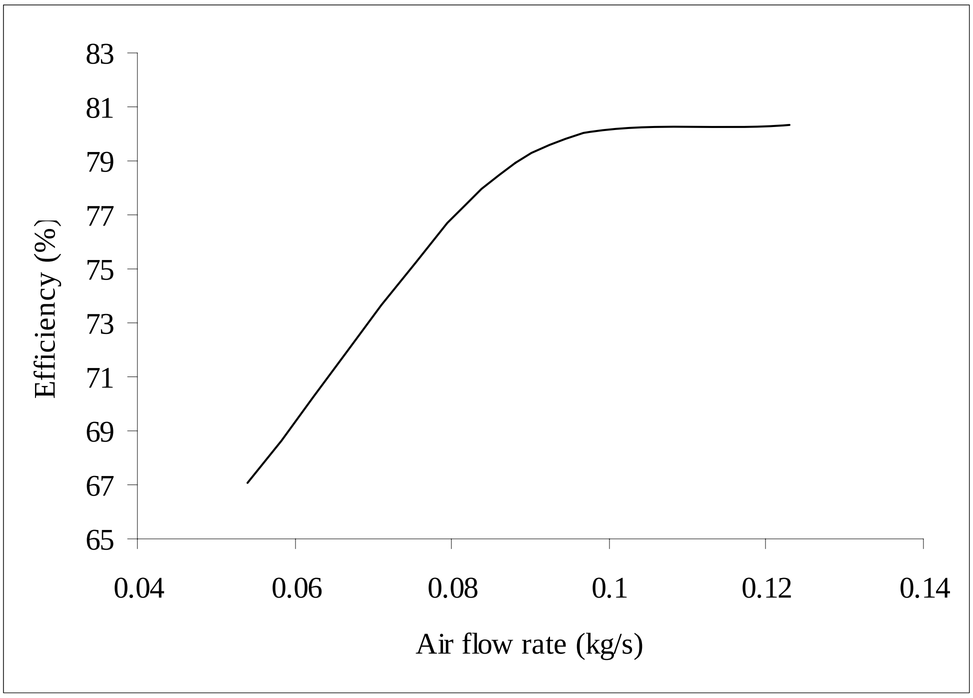

Fig. 4. Effect of air flow rate on maximum thermal efficiency

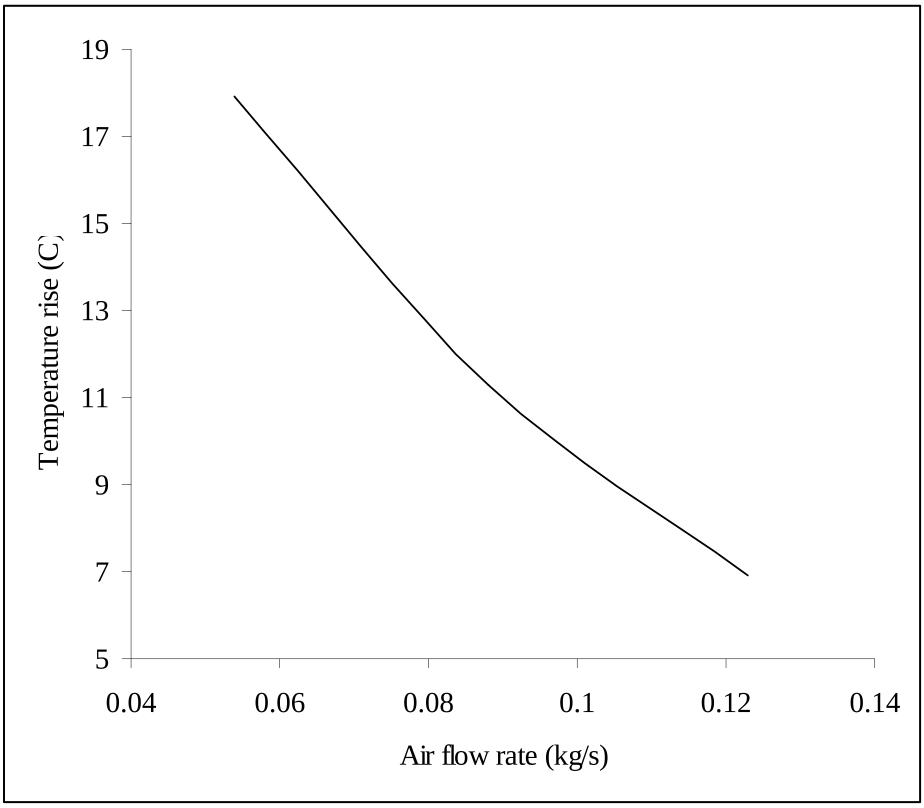

Fig. 5 Effect of air flow rate on temperature rise

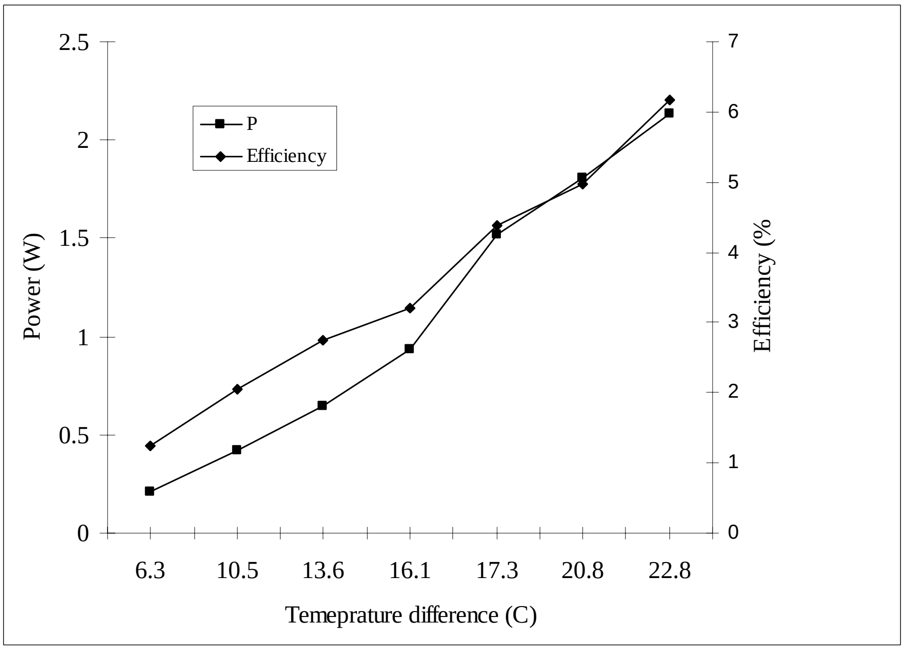

Fig. 6. Variation of power output and conversion efficiency with temperature difference.

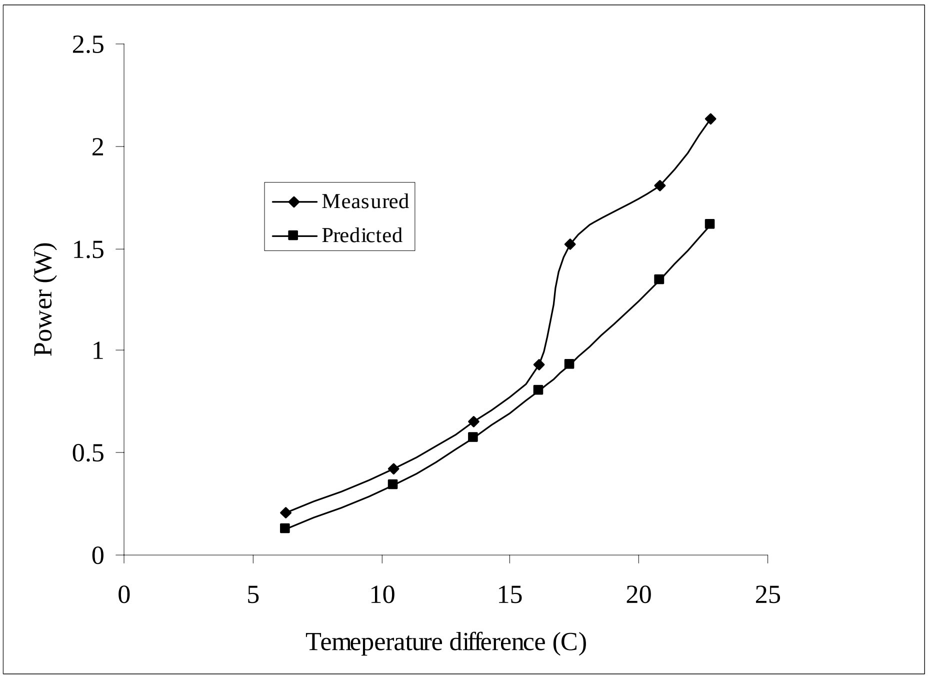

Fig. 7. Comparison between predicted and measured results.

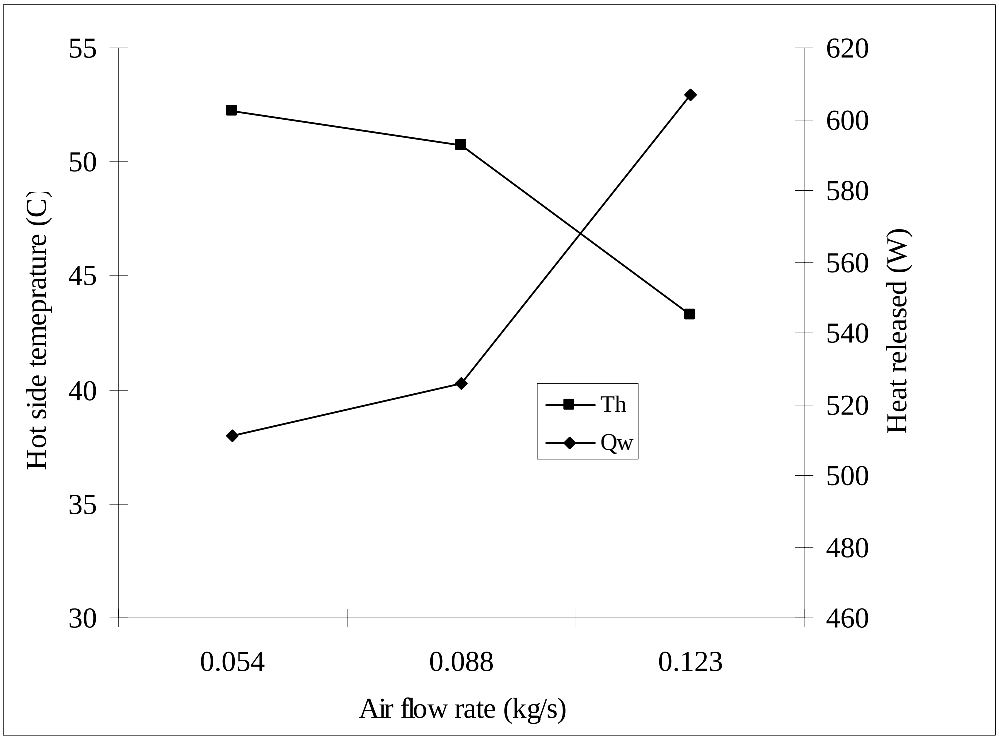

Fig. 8 Effect of air flow rate on the hot side temperature and heat released (Incident solar radiation of 650 W/m^2)

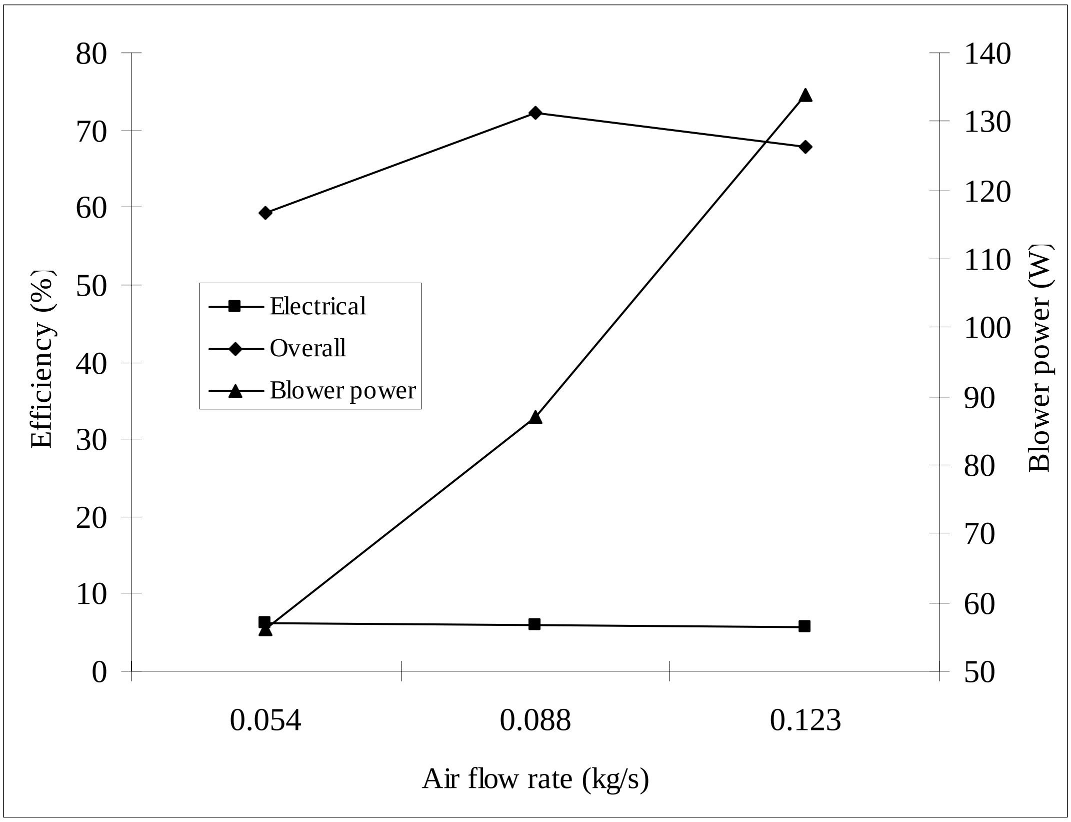

Fig. 9. Effect of air flow rate on overall and conversion efficiencies and blower power.